Journal of Inorganic Biochemistry 225 (2021) 111600

Contents lists available at ScienceDirect

Journal of Inorganic Biochemistry

journal homepage: www.elsevier.com/locate/jinorgbio

Copper(II)-*N*-hydroxy-*N,N′*-diarylformamidine complexes: Synthesis, crystal structures, antibacterial and molecular docking studies

Wisdom A. Munzeiwa [a,b], Segun D. Oladipo [a], Collins U. Ibeji [c], Chunderika Mocktar [d], Bernard Omondi [e,*]

[a] School of Chemistry and Physics, Westville Campus, University of Kwazulu-Natal, Private Bag X54001, Durban 4000, South Africa
[b] Chemistry Department, Bindura University of Science Education, P Bag 1020, Bindura, Zimbabwe
[c] Department of Pure and Industrial Chemistry, University of Nigeria, Nsukka, Nigeria
[d] Discipline of Pharmaceutical Sciences, School of Health Sciences, University of Kwazulu-Natal, Private Bag X54001, Durban 4000, South Africa
[e] School of Chemistry and Physics, Pietermaritzburg Campus, University of Kwazulu-Natal, Private Bag X01, Scottsville 3209, South Africa

ARTICLE INFO

Keywords:
Cu(II) complexes
N-hydroxy-*N,N′*-diarylformamidine
Antimicrobial
Molecular docking

ABSTRACT

A series of Cu(II) complexes were synthesized by using *N*-hydroxy-*N,N′*-diarylformamidine ligands: *N*-hydroxy-*N*, *N′*-(phenyl)formamidine (**L1**), *N*-hydroxy-*N′*-(4-methylphenyl)formamidine **(L2)**, *N*-hydroxy-*N,N′*-(2,6-dimethylphenyl)formamidine (**L3**), *N*-hydroxy-*N,N′*-(2,6-diisopropylphenyl)formamidine (**L4**). Reaction of ligands **L1**–**L4** with hydrated copper acetate furnished mononuclear Cu(II) complexes **1**–**4** with general formula [Cu-(**L**)$_2$]. The molecular structures of complexes **3** and **4**, as determined by single crystal X-ray diffraction, showed both to have square planar geometry with a near C_2 symmetry. The antimicrobial potency of all four complexes was evaluated against three gram-(–) bacteria (*S. typhimurium*, *P. aeruginosa,* and *E. coli)* and two gram-(+) bacteria (*Methicillin-resistant S. aureus (MRSA*) and *S. aureus*), with ciprofloxacin as the reference drug. All tested complexes were inactive against gram-(+) bacteria strains except for complex **1,** which displayed excellent activity when compared to the reference. Molecular docking studies showed that hydrogen bonding, pi-sigma and van der Waals interactions are prominent complex-protein connections, with complex **2** displaying good binding affinities with the studied biological targets.

1. Introduction

The continuous threats posed to human health by infectious diseases and the rapid development of multi-drug resistant microbial pathogens have in the last decade caused serious global health concerns [1,2]. By the year 2050, it is anticipated that the formidable challenge posed by increased antimicrobial resistance to known clinical drugs will have caused a total of 10,000,000 deaths from infectious disease [2,3]. An urgent global action plan has been flagged by the World Health Organisation (WHO), which calls for all countries to take measures against drug-resistant microbes and work towards the discovery of safer and efficacious new antimicrobial drugs [4,5]. Such drugs should have different mechanisms of action from those of well-known antimicrobial agents, to which relevant pathogens are resistant [6,7].

Copper(II) metal complexes synthesized from different ligands have in the past been tested as antimicrobial agents [8–11]. They have also been tested as corrosion inhibitors [12,13], antioxidants [14], antifungal [15,16] and anticancer agents [17,18]. The biological activities of *N*-hydroxyl-*N′*-diarylformamidines have been reported [19,20]. In this study they are used as ligands because we envisaged that their biological activities would be enhanced upon chelation with Cu(II) ions. It is known that the formation of metal chelates would increase their lipophilic character, thereby easing the permeability of these complexes through lipid layers of cell membranes [21]. Recently, our research group have reported the biological activities of metal complexes derived from both symmetrical and unsymmetrical *N,N′*-diarylformamidine derivatives [22,23]. To advance these studies, we have introduced a hydroxyl group (-OH) to the formamidines so as to afford metal complexes with nitrogen and oxygen binding atoms as bidentate systems, and we investigate if this might enhance their biological activities. Our interest stems from ligands with *O*, *N* or *S* binding atoms being frequently found in molecules of biological interests [24].

We, therefore, report the synthesis, structural characterization, *in vitro* antibacterial and computational studies of Cu(II)-*N,N′*-

* Corresponding author.
E-mail address: owaga@ukzn.ac.za (B. Omondi).

https://doi.org/10.1016/j.jinorgbio.2021.111600
Received 6 March 2021; Received in revised form 26 August 2021; Accepted 28 August 2021
Available online 3 September 2021

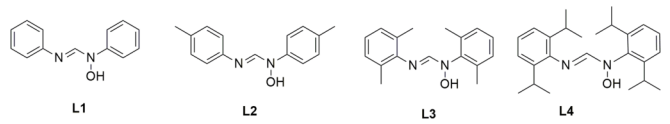

Fig. 1. *N*-hydroxy-*N,N′*-diarylformamidine ligands employed in the synthesis of complexes reported herein.

diarylformamidine complexes. The antibacterial potential of each of the metal complexes was evaluated against gram-positive bacterial strains *Methicillin-resistant S. aureus (MRSA*) and *S. aureus* and gram-negative bacterial strains *S. typhimurium, E. coli*, and *P. aeruginosa*.

2. Experimental section

2.1. Materials

All experiments were carried out under argon, 5.0 technical grade, (Airflex Industrial Gases, South Africa) using Schlenk techniques. All solvents were obtained from Sigma-Aldrich. Reagent grade absolute ethanol (98%) was distilled and dried from magnesium turnings; dichloromethane (DCM) (99%) and hexane (98%) were dried from a sodium benzophenone mixture. The reagents, $Cu(OAc)_2.H_2O$ (98%), and 3-chloroperoxybenzoic acid (*m*-CPBA) (77%), were also obtained from Sigma-Aldrich. Anhydrous $MgSO_4$ (98%), NaOH (99%), anhydrous $NaHCO_3$ (97%) and anhydrous K_2CO_3 (99%) were obtained from Promark Chemicals, South Africa.

2.2. Instrumentation

The melting point of the complexes was recorded using Electrothermal (9100) digital melting point apparatus. IR spectra were obtained from a PerkinElmer Universal ATR spectrum 100 FT-IR spectrometer. Mass spectra of the complexes were obtained from a Water synapt GR electrospray positive spectrometer. Elemental analyses were recorded on a Vario elemental EL cube CHNS analyzer.

3. General synthesis methods

3.1. Synthesis of N-hydroxy-N,N′-diarylformamidine ligands

Amidine (1.0 mmol) was dissolved in DCM and then solid sodium hydrogen carbonate (1.0 mmol) was added and the mixture cooled to 0 °C. Thereafter, *m*-CPBA (1.2 mmol) in DCM was added dropwise and the reaction mixture was allowed to warm to room temperature with stirring for a further 1 h. The reaction mixture was then washed with a solution of potassium carbonate (5%; 2 × 25 mL) and the combined organic fractions were dried over anhydrous magnesium sulphate and filtered. The solvent was then removed by evaporation to afford *N*-hydroxy-*N,N′*-(phenyl)formamidine (**L1**), *N*-hydroxy-*N,N′*-(4-methylphenyl)formamidine (**L2**), *N*-hydroxy-*N,N′*-bis(2,6-dimethyl) formamidine (**L3**), *N*-hydroxy-*N,N′*-bis(2,6-diisopropylphenyl)formamidine (**L4**) in the respective reactions. Ligand **L1** was obtained as an oil whilst **L2**, **L3** and **L4** were obtained as white solids (Fig. 1).

3.2. Synthesis of Cu(II) complexes

Copper(II) acetate (1 mmol) was dissolved in water and the pH adjusted to 8.0 using 1 M NaOH solution. Thereafter, a solution of the ligand (2.0 mmol) in aqueous ethanol (90%) was added. In each case, a precipitate was formed immediately, and the reaction mixture was stirred at room temperature for 8 h. Deionized water (100 mL) was added and then the temperature lowered to 4 °C with stirring for a further 2 h. The resultant solids were collected by filtration, washed first with hot water and then with aqueous ethanol (50%). The complexes were then dissolved in DCM, dried with anhydrous $MgSO_4$, filtered and by slow evaporation of the solvent, the desired products were obtained as solids.

Table 1
Summary of X-ray crystal data collection and structure refinement parameters for complexes **3** and **4.**

	3	**4**
Empirical formula	$C_{34}H_{38}CuN_4O_2$	$C_{50}H_{70}CuN_4O_2$
Formula weight	598.22	822.64
T(K)	173(2)	173(2)
λ(Å)	0.71073	0.71073
Crystal system	*Monoclinic*	*Triclinic*
Space group	$P21_{/c}$	*P-1*
a (Å)	8.6554(2)	10.5284(3)
b (Å)	8.4414(2)	10.8147(3)
c (Å)	20.6115(6)	11.7799(4)
α,	90	109.5950(10)
β,	91.4330(10)	105.149(2)
γ (°)	90	99.928(3)
V (Å^3)	1505.48(7)	1168.75(6)
Z	2	1
ρcalc (mg/m^3)	1.320	1.169
μ (mm^{-1})	0.762	0.508
F(000)	630	443
Crystal size (mm)	0.320 × 0.230 × 0.140	0.240 × 0.220 × 0.130
θ range for data collection (°)	1.977 to 27.514	1.954 to 27.492
Index ranges	$-11 \le h \le 9$ $-10 \le k \le 10$ $-22 \le l \le 26$	$-13 \le h \le 13$ $-13 \le k \le 14$ $-15 \le l \le 12$
Reflections collected	19,352	17,575
Independent reflections	3425 [R(int) = 0.0269]	5235 [R(int) = 0.0173]
Completeness to theta = 25.24° (%)	99.6	99.9
Data/restraints/parameters	3425/0/191	5235/0/267
Goodness-of-fit (GOF) on F^2	1.062	1.063
Final R indices [$I > 2\sigma(I)$]	$R1 = 0.0285$ w$R2 = 0.0760$	$R1 = 0.0284$ w$R2 = 0.0737$
R indices (all data)	$R1 = 0.0331$ $wR_2 = 0.0781$	$R1 = 0.0309$ $wR_2 = 0.0753$
Largest diff. peak and hole (e Å^{-3})	0.338 and −0.428	0.365 and −0.307

3.2.1. [Cu-(L1)$_2$] (1)

The reaction of ligand **L1** (0.30 g, 0.619 mmol) and $Cu(OAc)_2.2H_2O$ (0.087 g, 0.495 mmol) in ethanol furnished complex **1** as a brown powder. Yield 79%. Melting point: decomposes above 195 °C. IR υ (cm^{-1}): 3018 (w), 2922 (w), 1608 (s), 1586 (s), 1466 (m), 1362 (w), 1298 (w), 1205 (m), ESI-TOF MS: *m/z* (%) 508.0912 (100) [M + Na]$^+$. Elemental analysis for $C_{26}H_{22}CuN_4O_2$ (%): calculated C 64.25, H 4.56, N 11.53; found: C 64.33, H 4.85, N 11.49.

3.2.2. [Cu-(L2)$_2$] (2)

The reaction of ligand **L2** (0.30 g, 0.555 mmol) and $Cu(OAc)_2.2H_2O$ (0.084 g, 0.454 mmol) in ethanol furnished complex **2** as a brown powder. Yield 71%. Melting point: decomposes above 200 °C. IR υ (cm^{-1}): 3018 (w), 2990 (w), 1623 (s), 1614 (s), 1456 (m), 1390 (w), 1302 (w), 1206 (m), ESI-TOF MS: *m/z* (%) 541.1745 (100) [M + Na]$^+$. Elemental analysis for $C_{30}H_{30}CuN_4O_2$ (%): calculated: C 66.46, H 5.58, N 10.33; found: C 66.69, H 5.83, N 10.38.

3.2.3. [Cu-(L3)$_2$] (3)

The reaction of ligand **L3** (0.30 g, 0.788 mmol) and $Cu(OAc)_2.2H_2O$ (0.076 g, 0.394 mmol) in ethanol furnished complex **3** as a brown powder. Yield 76%. Melting point: decompose above 205 °C. IR υ (cm^{-1}): 3018 (w), 2918 (w), 1608 (s), 1583 (s), 1466 (m), 1390 (w), 1296 (w), 1205 (m), ESI-TOF MS: *m/z* (%) 621.32(100) [M + Na]$^+$. Elemental analysis for $C_{34}H_{38}N_4O_2Cu$ (%): calculated: C 63.05, H 6.50, N 8.40. found: C 62.79, H 6.83, N 8.82.

3.2.4. [Cu-(L4)$_2$] (4)

The reaction of ligand **L4** (0.30 g, 0.919 mmol) and Cu(OAc)$_2$.2H$_2$O (0.078 g, 0.394 mmol) in ethanol furnished complex **4** as a brown powder. Yield 76%. Melting point: decomposes above 238 °C. IR *ν* 3064 (w), 2960 (s), 2867 (w), 1664 (m), 1620 (s), 1461(m), 1326 (w), 1290 (w), 1254 (w). ESI-TOF MS: m/z (%) 844.6 (100) $[M + Na]^+$. Elemental analysis for $C_{50}H_{70}CuN_4O_2$: C (%): calculated: 73.00, H 8.58, N 6.81; found: C 73.15, H 8.53, N 6.78.

3.3. Single-crystal X-ray diffraction

Crystal evaluation and data collection for all samples were done on a Bruker Smart APEXII diffractometer with Mo Kα radiation ($I = 0.71073$ Å), equipped with an Oxford Cryostream low-temperature apparatus operating at 100 K. Reflections were collected at different starting angles and the *APEX*II program suite was used to index the reflections [25]. Data reduction was performed using the *SAINT* [26] software and the scaling and absorption corrections were applied using the *SADABS* [27] multi-scan technique. The structures were solved by the direct method using the *SHELXS* program and refined using *SHELXL* program [28]. Graphics of the crystal structures were drawn using OLEX^2 software [29]. Non-hydrogen atoms were first refined isotropically and then by anisotropic refinement with the full-matrix least-squares method based on F^2 using *SHELXL* [28]. The crystallographic data and structure refinement parameters for complexes **3** and **4** are given in Table 1.

3.4. In vitro antimicrobial studies

The antimicrobial activity of the Cu(II) complexes **1**–**4** were evaluated against three gram-negative bacteria, *viz*: *S. typhimurium* ATCC 14026, *P. aeruginosa* ATCC 27853, and *E. coli* ATCC 25922, and two gram-positive bacteria, *viz*: *Methicillin-resistant S. aureus (MRSA)* ATCC 700699 and *S. aureus* ATCC 25923. Ciprofloxacin was used as a standard antibiotic for comparison while dimethyl sulfoxide (DMSO) was used as a negative control, in which it showed no antibacterial activity against any of the bacterial strains used for this study at the different concentrations. The samples were prepared by dissolving 1000 μg of the test sample in 1 mL of DMSO. The bacteria were inoculated onto nutrient agar (NA) (Biolab, South Africa) plates using the streak plate technique and incubated at 37 °C for 18 h [30]. A single colony was isolated and inoculated into 10 mL sterile nutrient broth (NB) (Biolab, South Africa). This was incubated at 37 °C for 18 h in a shaking incubator (100 rpm). The concentration of each bacterial strain was adjusted with sterile distilled water to achieve a final concentration equivalent to 0.5 McFarland Standard (i.e 1.5×10^8 cfu/mL) using a densitometer (McFarland Latvia) [31]. Thereafter, the Mueller–Hinton agar (MHA) plates were lawn inoculated with the diluted bacteria using a sterile throat swab. After 5 μL of each sample had been spotted onto the MHA plates, the plates were incubated at 37 °C for 18 h and then assessed for antibacterial activity, which was denoted by a clear zone at the point of spotting. Samples that showed antimicrobial potential during antibacterial screening were tested further to determine their minimum inhibitory concentration (MICs). In this determination, the samples were serially diluted 10 times to achieve concentrations ranging from 1000 μg/mL to 0.2 μg/mL. For the samples where MICs had been lower than 0.2 μg/mL, the solutions were further diluted serially 5 times to achieve concentrations ranging from 0.100 μg/mL to 0.00625 μg/mL. Then 5 μL of each sample at the different concentrations was spotted onto the MHA plates and the plates were incubated at 37 °C for 18 h and then assessed for their MIC [32]. These tests were done in triplicate and the MIC was determined as the lowest concentration of the complexes at which no visible bacterial growth could be observed after incubation.

3.5. Molecular docking method

The molecular docking technique was carried out in this study to investigate the inhibitory potentials *via* calculated binding energies. The 3D crystal structures of proteins were retrieved from the protein data bank (PDB). The proteins of *S. aureus*, *E. coli*, *P. aeruginosa* were identified with their PDB codes 2DHN (2.2 Å resolution) [32], 1wxh (1.97 Å resolution) [33], 2w7q (1.88 Å resolution) [34], respectively. The grid box size was determined using AutoDock tools [35] 1.5.4 for the binding site as derived from the corresponding reference complexes and the dimension applied for docking was X = 24 Y = 24 Z = 24 with 1.00 Å as the grid spacing [36]. Gasteiger charges were added using the AutoDock Tools graphical-user-interface from MGL Tools [37]. The Lamarckian genetic algorithm was applied in the search for the optimum binding site for the ligands. The ligands were optimized before docking using Gaussian 09 [38], to achieve the global minimum.

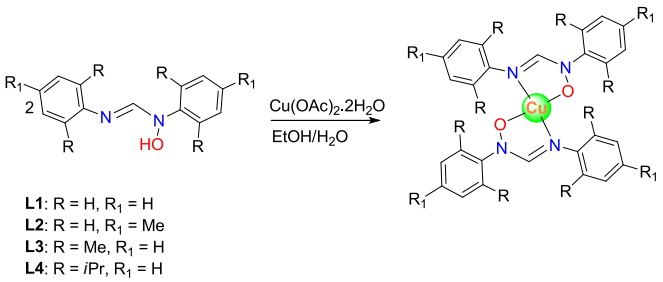

Scheme 1. Synthesis of Cu(II) *N*-hydroxy-*N,N′*-diarylformamidine complexes.

Table 2
IR azomethine (C=N) symmetry stretch frequency for ligands and complexes, respectively.

Complex	IR υ(C=N) cm^{-1}		
	Ligand	Complex	Δv
1	1608	1586	22
2	1623	1614	9
3	1620	1610	10
4	1612	1608	4

4. Result and discussion

4.1. Synthesis of N-hydroxy-N,N′-diarylformamidine ligands and their Cu (II) complexes

The ligands **L1** – **L4** were synthesized *via* one-step oxidation of *N,N′*-diarylformamidine precursors [39] using slight modifications of a method in the literature [40]. Bis-ligated copper complexes [Cu-(**L1**)$_2$] (**1**), [Cu-(**L2**)$_2$] (**2**), [Cu-(**L3**)$_2$] (**3**), [Cu-(**L4**)$_2$] (**4**) were obtained as brown solids with excellent yield (75–84%) (Scheme 1) by reacting copper acetate and the ligands in 2:1 metal:ligand ratio.

The complexes decomposed between 195 °C and 245 °C, with the trend being influenced by substituents on the phenyl ring. The microanalytical data was consistent with the molecular structure, which showed a metal:ligand ratio of 1:2. This was further complemented by mass spectrometry data for the complexes with spectra exhibiting *m/z* signals corresponding to the parent complex as sodium adducts (Fig. S1a–d).

4.2. Spectroscopy studies

4.2.1. Fourier transform infrared (FT-IR) spectroscopy

The IR spectra of complexes **1**–**4** showed a general shift of the azomethine (C(H)=N) symmetric vibrations to lower frequencies compared to ligands, which alludes to the participation of the imine nitrogen in metal coordination. For example, the C=N symmetric stretching vibrations in complex **1** appeared at 1612 cm^{-1} as compared to 1619 cm^{-1} in ligand **L1**. The characteristic positive shifts are a result of the

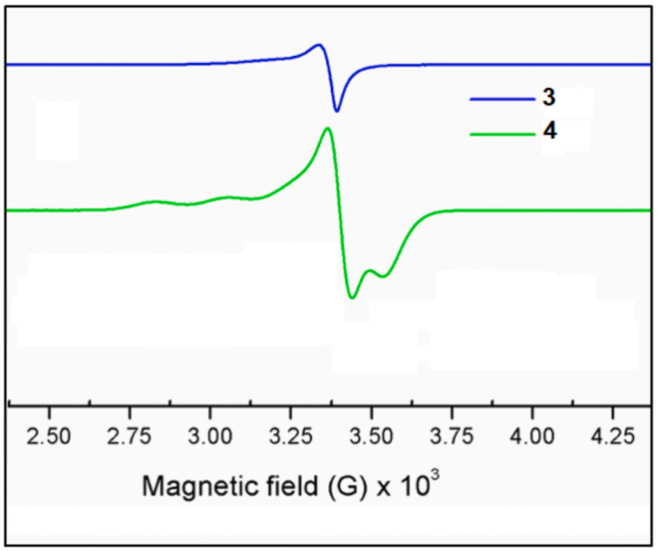

Fig. 2. Solid state EPR spectrum of complexes 3 and 4 (295 K, 9.786GHz).

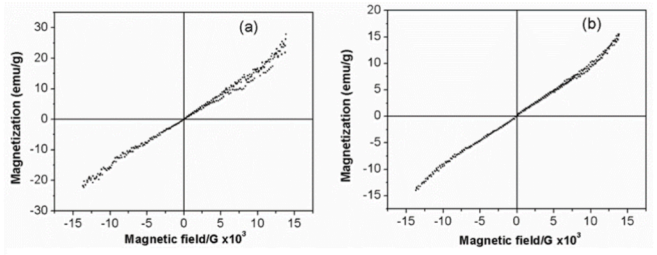

Fig. 3. Magnetization behaviour of complexes 3 and 4.

migration of the imidine bridge π-electron density towards the metal centre conferring partial bond character on the C═N bond, leading to vibration at lower frequencies [42]. The summarized data of shifts for other complexes are shown in Table 2.

4.2.2. Electron paramagnetic resonance (EPR) studies of complexes 3 and 4

To further infer the solid-state electronic structure of the copper complexes, X-band EPR spectra of selected complexes were acquired at 295 K (Fig. 2). The EPR spectra of complexes **3** and **4** are perfectly isotropic with a single line (g = 2.1082). This infers that there is a completely symmetric environment where the electrons in separate d-orbitals interact in all directions (identical g-factors). The broad signals and slight deviation of the g-factors from the free electron value (2.0023) points to the $d_{(x2-y2)}$ orbital (B_{1g}) ground state occupancy by the unpaired Cu(II) electrons. The g-values are comparable to those of other square-planar complexes reported in literature [41]. The EPR spectra also showed a resolved hyperfine structure in the perpendicular section due to the interaction of metal electrons with nitrogen atoms. The spectra for all the complexes are devoid of $m_s = \pm 2$ transitions a half field signal ruling out any meaningful Cu···Cu interactions.

4.3. Magnetic studies of complexes 3 and 4

The paramagnetic nature of the Cu(II) complexes was further confirmed by magnetic studies. Fig. 3 shows almost linear hysteresis loops and magnetization does not reach saturation, even at higher applied magnetic field. This is because of the paramagnetic nature of Cu (II) ions and their magnetic moments being aligned with the magnetic field. The coercivity values range from 21.8–89.7 H_{ci} and magnetization lies between 10.35 and 25.9 M_s. These low values are characteristic of a soft magnet and strong short-range correlation.

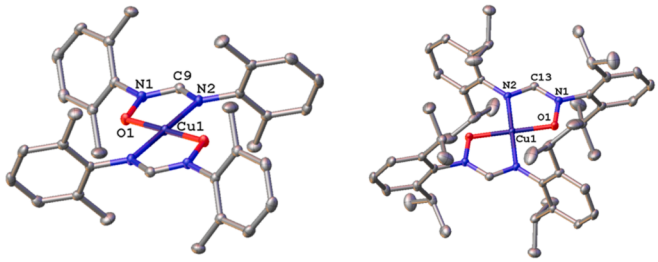

Fig. 4. X-ray crystal structure of complexes **3** and **4** with thermal ellipsoids drawn at 50% probability level and hydrogen atoms having been omitted for clarity.

Table 3
Selected bond lengths and angles for complexes **3** and **4**.

	3	**4**
Bond lengths [Å]		
M—N	1.9138(10)–1.9385(12)	1.9350(10)–1.9351(10)
M—O	1.9138(10)	1.9185(9)
C—N	1.9385(12)	1.3135(16)–1.3119(16)
Bond angles [°]		
O—M—N(cone)	83.59(5)–96.41(5)	95.96(4)–84.04(4)
O—M—O	180.0	180.0
N—M—N	180.0	180.0
Torsion angles [°]		
C—N—O—M	−1.58(15)	−0.40(12)
N—C—N—M	0.23(17)	0.34(14)
2,6-R-Ph-(NO)	60.21(17)	93.69(13)

Table 4
Minimum inhibitory concentration of the metal complexes (μg/mL).

Complexes	Gram (−) bacteria			Gram (+) bacteria	
	E. coli	*S. typhimurium*	*P. aeruginosa*	*S. aureus*	*MRSA*
1	0.20	NA	0.10	6.25	12.50
2	0.80	NA	0.20	NA	NA
3	6.25	NA	1000	NA	NA
4	100	NA	1000	NA	NA
Ciprofloxacin[a]	0.20	0.40	0.80	25	25

NA = No activity
[a] Standard.

4.4. X-ray structural analysis

Perspective views of complexes **3** and **4** are illustrated in Fig. 4 and selected bond lengths and angles are recorded in Table 3. Complexes **3** and **4** are supported by symmetrical *N,N*-hydroxy formamidine ligands and good quality crystals of both complexes were obtained by slow diffusion of diethyl ether into their saturated dichloromethane solution. The asymmetric units of both complexes contain half complex molecules, with the other half being generated through inversion centres. The complex molecule contains a metal ion that is *bis*-ligated *via* the imine nitrogen and hydroxyl oxygen, and the acetate auxiliary ligands are completely excluded from the coordination sphere. The donor atom connectivity results in penta-metallacycles, which are similar to other *N, O* bidentate ligands [42]. The Cu atoms also adopt a square planar geometry with bond angles of 83.59(5) – 96.41(5)°. Steric repulsion between the bulky 2,6-^{i}Pr groups resulted in greater tilt angles in **4** as compared to **3**. The Cu—O and Cu—N bond distances are almost comparable in both complexes, and they lie between 1.9139(10) and 1.9384 (10) Å. Similar values have been reported in the literature for related

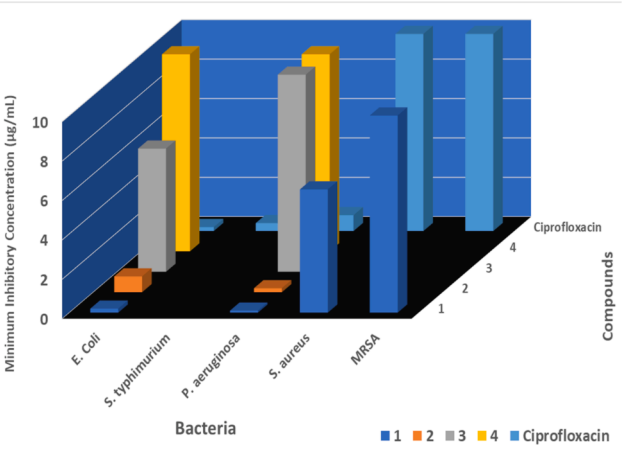

Fig. 5. Minimum inhibitory concentration (MIC) of the metal complexes *vs* bacteria. *The blank spaces represent no activity (NA) and 10 for MIC values of ≥12.5 µg/mL.

Table 5
Binding free energies (ΔG) in kcal/mol of complexes with different targets obtained using AutoDock 1.5.4.

Complex	*S. aureus*	*E. coli*	*P. aeruginosa*
1	−5.4	−5.3	−5.2
2	−7.4	−5.0	−5.4
Ciprofloxacin[a]	5.3	5.1	5.2

structures [43,44].

4.5. Antimicrobial activities evaluation

Complexes **1**–**4** together with ciprofloxacin as a standard were screened against five bacteria strains and the results are presented in Table 4 and Fig. 5. The *in vitro* antibacterial evaluation based on MIC values showed that some of the complexes could inhibit the growth of all the tested bacteria strains effectively, except *S. typhimurium*. All the complexes were inactive against gram-(+) bacteria strains (*S. aureus* and *MRSA*) except complex **1,** which displayed excellent activity when compared to ciprofloxacin (reference drug) with MIC values of 6.25 µg/mL and 12.50 µg/mL against *S. aureus* and *MRSA* (Fig. 5). This showed that complex **1** is 3-fold and 2-fold more potent against *S. aureus* and *MRSA*, respectively, when compared to ciprofloxacin. We found *S. typhimurium* was non-susceptible to all the complexes. The failure of the complexes **2**–**4** to inhibit *S. aureus* and *MRSA* strains and all the complexes to inhibit *S. typhimurium* could be as a result of the inability of the compounds to penetrate through the bacterial cell wall or the complexes might have been modified or rendered inactive as they entered the cell wall [45]. Complexes **3** and **4** displayed the least activity against *P. aeruginosa*, being effective at only the highest concentration (1000 µg/mL), whilst complexes **1** and **2** displayed better activity relative to ciprofloxacin. Complexes **1** and **2** are 3-fold and 2-fold, repectivley, more active than the reference drug. All the complexes were active against *E.coli,* with **2**, **3** and **4** showing moderate activity and complex **1** having the same activity as the reference drug (ciprofloxacin). Among all the complexes, we can speculate that complex **1** showed a broad spectrum of effectiveness and the presence of alkyl substituents did not increase the antimicrobial activity of the complexes.

4.6. Molecular docking

The docking studies simulation was carried out to give insight into the inhibitory potential of metal complexes to target proteins *via* their binding affinities. The binding energies of complexes **1** and **2** obtained give insight into the thermodynamical feasibility of the different binding interactions. As displayed in Table 5, complex **2** showed the highest binding affinity with *S. aureus* compared to **1** and the reference drug. Complexes **1** and **2** showed reasonable activity to *E. coli* and *P. aeruginosa* compared to the reference drug. The docking simulation obtained in this study displayed hydrogen bonding, pi-sigma, and van

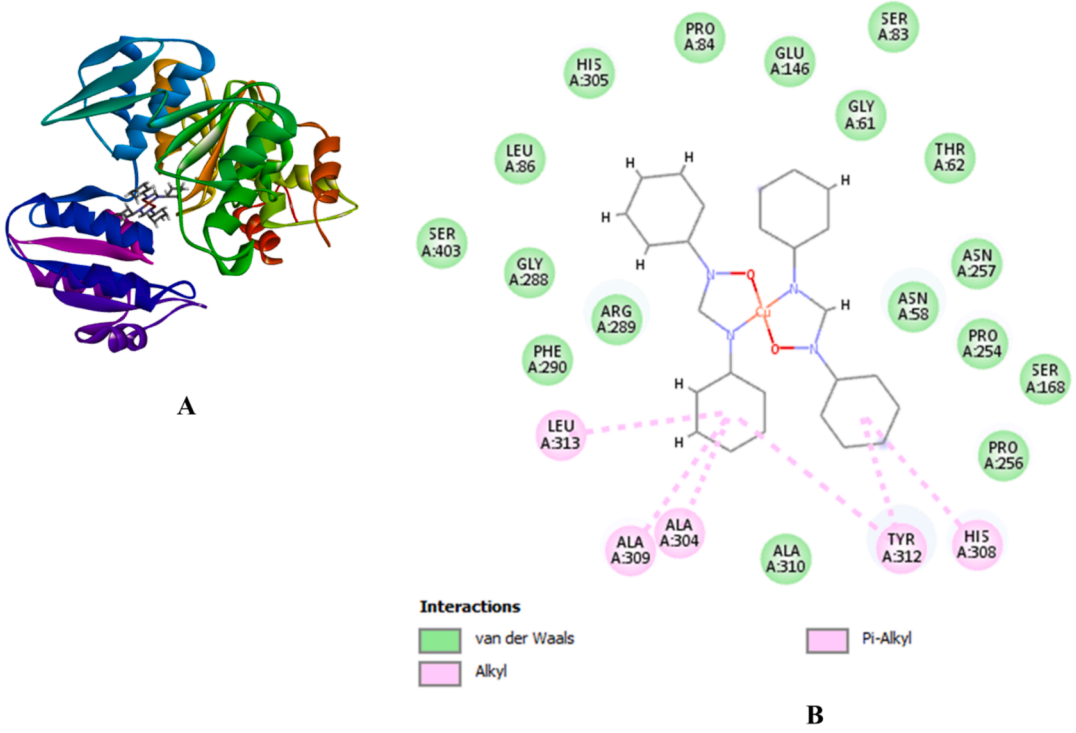

Fig. 6. Pictorial description of the 3-D complex **1** (A) in the binding pocket of *E. coli* and 2-D, (B) The interactions with amino acid residues inside the active pocket of *E. coli.*

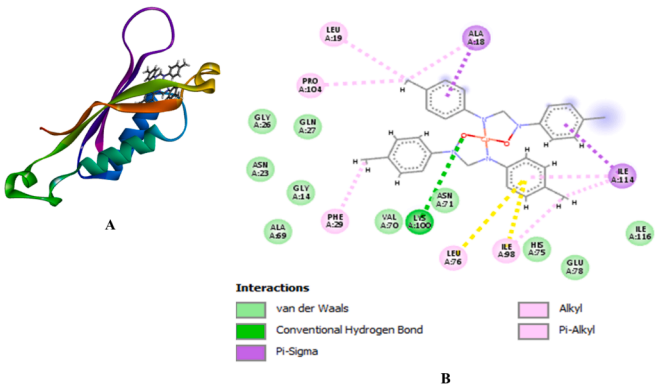

Fig. 7. A pictorial description of the 3-D complex **2** (A) in the binding pocket of *S. aureus (highest binding affinity)* and (B) 2-D, The interactions with amino acid residues inside the active pocket of *S. aureus*.

der Waals interactions, which explain the relative strength of metal-ligand bonding with selected biological targets (Fig. 6 and Fig. 7). Complex **2** displayed good hydrogen bonding interaction with the active site of amino acid residue (LYS100) of *S. aureus*, compared with other studied biological targets. It showed more thermodynamically favourable interactions with the molecular targets as evidenced by the binding energies and 2D interactions. Complex **1** showed little interaction with amino acid residues of *E. coli* indicating insignificant binding abilities. Complexes **3** and **4** showed no binding as both metal complexes could not bind around the active sites of the studied target proteins. It was also observed that the reference drug used (ciprofloxacin) interacted with the target proteins with comparable binding energies. The interactions obtained in this study give insight into the probable mechanism of inhibition that would ultimately lead to the inactivation of the bacterial cells and the subsequent death of the organism colonies. The results of the docking studies agreed with the antimicrobial results obtained.

5. Conclusion

Cu(II) complexes of N-hydroxy-*N,N′*-diarylformamidine were synthesized and characterized by FT-IR, mass spectrometry and elemental analysis. The X-ray structural analysis of **3** and **4** showed that the Cu(II) atom is bonded by two nitrogen atoms and two oxygen atoms from the two *N*-hydroxy-*N,N′*-diarylformamidine ligands to form penta-metallacycles, with the Cu(II) atom adopting square planar geometry. The *in vitro* antibacterial screening and the MICs showed that, while other complexes were moderately active or showed no activity, complex **1** had good antimicrobial activities against all the bacterial strains except *S. typhimurium*, and displayed even better activity than did ciprofloxacin. Molecular docking studies verified that the complex-proteins interactions are spontaneous as a result of hydrogen bonding, pi-sigma, and van der Waals interactions.

Declaration of Competing Interest

There are no conflicts of interest.

Acknowledgements

The authors acknowledge the College of Agriculture, Science and Engineering, University of KwaZulu-Natal (UKZN), and the National Research Foundation (NRF), South Africa for financial support and CHPC (www.chpc.ac.za) for computational resources.

Appendix A. Supplementary data

Supplementary data to this article can be found online at https://doi.org/10.1016/j.jinorgbio.2021.111600.

References

[1] I. Levin-Reisman, I. Ronin, O. Gefen, I. Braniss, N. Shoresh, N.Q. Balaban, Science. 355 (2017) 826–830.
[2] L.-L. Wang, N. Battini, R.R.Y. Bheemanaboina, S.-L. Zhang, C.-H. Zhou, Eur. J. Med. Chem. 167 (2019) 105–123.
[3] M. Sprenger, K. Fukuda, Science. 351 (2016) 1263–1264.
[4] E.D. Brown, G.D. Wright, Nature. 529 (2016) 336–343.
[5] L.L. Silver, Clin. Microbiol. Rev. 24 (2011) 71–109.
[6] A. Coates, Y. Hu, R. Bax, C. Page, Nat. Rev. Drug Discov. 1 (2002) 895–910.
[7] S.D. Oladipo, F.A. Olotu, M. Soliman, C. Mocktar, B. Omondi, J. Mol. Struct. 1219 (2020) 128553.
[8] A. Valent, M. Melník, D. Hudecová, B. Dudová, R. Kivekäs, M.R. Sundberg, Inorg. Chim. Acta 340 (2002) 15–20.
[9] N.V. Loginova, V. Tat'yana, R.A. Zheldakova, N.P. Osipovich, V.L. Sorokin, G. I. Polozov, G.A. Ksendzova, G.K. Glushonok, A.A. Chernyavskaya, O.I. Shadyro, Bioorg. Med. Chem. Lett. 16 (2006) 5403–5407.
[10] Z.H. Chohan, K.M. Khan, C.T. Supuran, Appl. Organomet. Chem. 18 (2004) 305–310.
[11] S.D. Oladipo, B. Omondi, C. Mocktar, Polyhedron. 170 (2019) 712–722.
[12] V.P. Singh, P. Singh, A.K. Singh, Inorg. Chim. Acta 379 (2011) 56–63.
[13] M. Mahdavian, M. Attar, Corros. Sci. 51 (2009) 409–414.
[14] H.-L. Wu, J.-K. Yuan, Y. Bai, F. Jia, B. Liu, F. Kou, J. Kong, Transit. Met. Chem. 36 (2011) 819–827.
[15] Z.H. Chohan, H. Pervez, A. Rauf, K.M. Khan, C.T. Supuran, J. Enzyme Inhib, Med. Chem. 19 (2004) 417–423.
[16] K. Alomar, A. Landreau, M. Allain, G. Bouet, G. Larcher, J. Inorg. Biochem. 126 (2013) 76–83.
[17] Z. Afrasiabi, E. Sinn, J. Chen, Y. Ma, A.L. Rheingold, L.N. Zakharov, N. Rath, S. Padhye, Inorg. Chim. Acta 357 (2004) 271–278.
[18] M. Collins, D. Ewing, G. Mackenzie, E. Sinn, U. Sandbhor, S. Padhye, S. Padhye, Inorg. Chem. Commun. 3 (2000) 453–457.
[19] C. Anastasi, O. Hantz, E. De Clercq, C. Pannecouque, P. Clayette, N. Dereuddre-Bosquet, D. Dormont, F. Gondois-Rey, I. Hirsch, J.-L. Kraus, J. Med. Chem. 47 (2004) 1183–1192.
[20] S. Delarue, S. Girault, F.D. Ali, L. Maes, P. Grellier, C. Sergheraert, Chem. Pharm. Bull. 49 (2001) 933–937.
[21] R.S. Joseyphus, M.S. Nair, Mycobiology. 36 (2008) 93–98.
[22] S.D. Oladipo, B. Omondi, C. Mocktar, Appl. Organomet. Chem. 34 (2020), e5610.
[23] S.D. Oladipo, C. Mocktar, B. Omondi, Arab. J. Chem. 13 (2020) 6379–6394.
[24] N. Nawar, N.M. Hosny, Chem. Pharm. Bull. 47 (1999) 944–949.
[25] Bruker, APEXII Bruker, AXS Inc, Madison, Wisconsin, USA, 2009.
[26] Bruker, SAINT Bruker, AXS Inc, Madison, Wisconsin, USA, 2009.
[27] Bruker, SADABS Bruker, AXS Inc, Madison, Wisconsin, USA, 2009.
[28] G. Sheldrick, Acta Crystallogr. Sect. A: Found. Crystallogr. 64 (2008) 112–122.
[29] O.V. Dolomanov, L.J. Bourhis, R.J. Gildea, J.A.K. Howard, H. Puschmann, J. Appl. Crystallogr. 42 (2009) 339–341.
[30] H. Govender, C. Mocktar, N.A. Koorbanally, J. Heterocycl. Chem. 55 (2018) 1002–1009.
[31] O.S. Aremu, K. Gopaul, P. Kadam, M. Singh, C. Mocktar, P. Singh, N. A. Koorbanally, Anticancer Agents Med. Chem. 17 (2017) 719–725.
[32] M. Hennig, D. Allan, I.C. Hampele, M.G. Page, C. Oefner, G.E. Dale, Nat. Struct. Mol. Biol. 5 (1998) 357.
[33] R. Jauch, A. Humm, R. Huber, M.C. Wahl, J. Biol. Chem. 280 (2005) 15131–15140.
[34] K. Remans, K. Pauwels, P. van Ulsen, L. Buts, P. Cornelis, J. Tommassen, S. N. Savvides, K. Decanniere, P. Van Gelder, J. Mol. Biol. 401 (2010) 921–930.
[35] M.F. Sanner, J. Mol. Graph Model. 17 (1999) 57–61.
[36] B. Yang, F. Hao, J. Li, D. Chen, R. Liu, J. Photochem. Photobiol. B 128 (2013) 35–42.
[37] G.M. Morris, R. Huey, W. Lindstrom, M.F. Sanner, R.K. Belew, D.S. Goodsell, A. J. Olson, J. Comput. Chem. 30 (2009) 2785–2791.
[38] M. Frisch, G. Trucks, H.B. Schlegel, G. Scuseria, M. Robb, J. Cheeseman, G. Scalmani, V. Barone, B. Mennucci, G. Petersson, Gaussian, Inc, Wallingford CT, 2009.
[39] M.L. Cole, G.B. Deacon, C.M. Forsyth, K. Konstas, P.C. Junk, Dalton Trans (2006) 3360–3367.
[40] M. Cibian, S. Derossi, G.S. Hanan, Dalton Trans. 40 (2011) 1038–1040.
[41] D.J. Hodgson, Inorg. Chim. Acta 75 (1983) 225–228.
[42] R. Murakami, T. Ishida, S. Yoshii, H. Nojiri, Dalton Trans. 42 (2013) 13968–13973.
[43] M. Cibian, S. Langis-Barsetti, J.G. Ferreira, G.S. Hanan, Eur. J. Inorg. Chem. 2016 (2016) 177–185.
[44] A. Okazawa, Y. Nagaichi, T. Nogami, T. Ishida, Inorg. Chem. 47 (2008) 8859–8868.
[45] E.M. Njogu, B. Omondi, V.O. Nyamori, J. Mol. Struct. 1135 (2017) 118–128.